Calculation of Couplings and Energy−Transfer Pathways between the Pigments of LH2 by the ab Initio Transition Density Cube Method

ARTICLE *in* THE JOURNAL OF PHYSICAL CHEMISTRY B · NOVEMBER 1998

Impact Factor: 3.3 · DOI: 10.1021/jp9811171

Calculation of Couplings and Energy-Transfer Pathways between the Pigments of LH2 by the ab Initio Transition Density Cube Method

Brent P. Krueger, Gregory D. Scholes, and Graham R. Fleming*

Department of Chemistry, University of California, and Physical Biosciences Division, Lawrence Berkeley National Laboratory, Berkeley, California 94720

Received: February 12, 1998; In Final Form: April 16, 1998

A practical method for accurate evaluation of the Coulombic contribution to the electronic coupling for energy transfer at any donor−acceptor separation is reported. The method involves the exact interaction between transition densities of each chromophore which are calculated ab initio and may include electron correlation. The method is used to calculate coupling strengths between the pigments of the bacterial light-harvesting complex, LH2, and to compare with results using the ideal dipole approximation (IDA). The results suggest that the relatively symmetric transitions of bacteriochlorophyll *a* (Bchla) pigments are reasonably well described by the IDA for separations >15 Å, although deviations are significant at smaller separations. The less symmetric transition of the twisted carotenoid pigment is rather poorly described by the IDA and shows significant deviation even at separations of well over 20 Å. The calculated coupling strengths are combined with estimates of the spectral overlap integral to estimate energy-transfer rates and time scales. The total depopulation time scale of the carotenoid S_2 state is estimated to be 85 fs, in reasonable agreement with experiment. The B800−B850 transfer time is estimated to be 1.3 ps (a factor of 2 slower than experiment). Rapid (<400 fs) B800−B800 energy transfer is also predicted. Moreover, the calculations suggest that energy flows both from the carotenoid and the B800 Bchla into pigments of several different protomer units, indicating that interaction between protomer units is important in the LH2 function.

1. Introduction

All photosynthetic systems share a structure in which a reaction center (RC) is surrounded by a network of antenna pigments.[1−4] This construction allows the organism to expand both the spatial and spectral cross-sections of the RC. However, this also means that excitation energy absorbed by antenna pigments must visit many molecules before reaching the RC. The transfer efficiency of each of these steps is critical to the efficient functioning of the photosystem.

Recent elucidation of the crystal structure of bacterial light-harvesting antenna[5,6] has allowed detailed examination of the coupling strengths and, therefore, EET rates between various pigments present in the antenna. For example, combining Förster theory and known structural parameters (separation and orientation) with time-resolved data can result in a microscopic picture of biological function.[7,8]

A key parameter in such examinations is the electronic coupling (between donor and acceptor) which promotes the energy transfer.[9−15] At donor−acceptor separations beyond their van der Waals radii, the coupling is described primarily by a Coulombic interaction between the transition densities of the chromophores.[9,15] For electronically allowed emission and absorption transitions, an interaction between dipole transition moments is generally applied.[16] This is the *ideal dipole approximation* (IDA), in which the dipole transition moment of each molecule is assumed to be very small compared to the molecular separation. For the absorption or emission of light, the IDA is an excellent approximation because the wavelength of light is much larger (several hundred times) than the size of the molecule, meaning that light is insensitive to any variations in the vector potential which may be present over the spatial extent of the transition density. However, when calculating the interaction between two molecules that are close together and exchange a virtual rather than real photon, the asymmetric shape and/or large spatial extent of the transition densities may make the IDA invalid. Likewise, if the transition is forbidden or only weakly allowed by dipole selection rules, the IDA will be invalid. In these situations the IDA is not viable because the transition dipole is a poor representation of the transition density.

In photosynthetic systems, deviation from the IDA has been under scrutiny as the sizes of the chromophores involved, $l \sim 9$ Å for bacteriochlorophyll *a* (Bchla) and $l \sim 25$ Å for rhodopin−glucoside (RG), are not small compared to their separation ($R \sim 15$ Å). (The IDA is valid only when $R \gg l$.) Some researchers have examined this deviation by reducing the transition density to transition "monopoles" distributed on atomic centers. These monopoles provide a molecular picture of the transition density that *approximately* accounts for its shape and size.[17,18] However, as with Mulliken population analysis, for example, the reduction scheme is not unique. Reduction of the transition density to atomic monopoles represents a significant loss of information. For example, the transition densities used here for Bchla have ∼500 000 data points throughout the three-dimensional space within and around the chromophore; in contrast, the monopole representation of Bchla has ∼80 data points, restricted to the approximately two-dimensional space of the molecule. In this work, we present a new method for calculating the Coulombic coupling that accounts for the shape of the transition density and is valid at all separations. The method utilizes transition density cubes (TDCs), represented in Figure 1, which can, in principle, account *exactly* for the shape and size of the transition density. We apply the method to

S1089-5647(98)01117-1 CCC: $15.00
Published on Web 06/12/1998

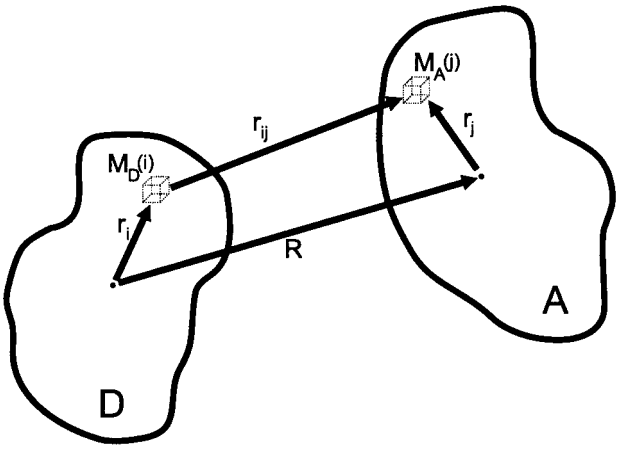

Figure 1. Depiction of two cells in the arbitrary donor (D) and acceptor (A) transition densities. The positions of TDC elements $M_D^{eq}(i)$ and $M_A^{eq}(j)$ are defined by vectors $\mathbf{r}_i$ and $\mathbf{r}_j$, respectively, relative to the centers of D and A. **R** gives the center-to-center separation and r_{ij} the separation between cells.

estimate coupling between Bchla and RG pigments in the peripheral light-harvesting antenna (LH2) of photosynthetic bacteria.

2. Coulombic Couplings and Transition Densities

In the present work, we investigate the general coupling between donor and acceptor transition densities which mediates EET at separations where there is no appreciable orbital overlap. We refer to this interaction as a Coulombic interaction in the sense that, in the following model involving four electrons and four orbitals, it has the form[12,15]

$$V^{\mathrm{Coul}} = 2\int d'(1)\, a(2) r_{12}^{-1} d(1)\, a'(2)\, \mathrm{d}\tau \equiv 2(d'd|aa') \tag{1}$$

where d represents donor orbitals, a acceptor orbitals, a prime designates an orbital that is unoccupied in the electronic ground state, and $1/r_{12}$ represents the Coulombic repulsion between electrons 1 and 2. In other words, the two-electron integral of eq 1 is an electrostatic interaction between the transition densities of the donor and acceptor. The transition density of molecule N is given by

$$M_N^{\mathrm{eq}}(\mathbf{r}) = \int_s \Psi_{N\mathrm{g}} \Psi^*_{N\mathrm{e}}\, \mathrm{ds}\, \mathrm{d}\mathbf{r} \tag{2}$$

where $\Psi_{N\mathrm{g}}$ and $\Psi_{N\mathrm{e}}$ denote the electronic ground and excited states of molecule N, respectively, and the integral is over only spin. The electrostatic term of eq 1 is the primary contributor to the Coulombic interaction. (Throughout this work we use the term Coulombic to refer to the interaction given above because in the usual form (see eq 3) it bears close resemblance to the classical, Coulombic interaction of two electrostatic dipoles. More strictly, this could be termed a resonance−Coulombic interaction to separate it from other interactions, such as exchange, which are Coulombic in nature but which do not share the Förster resonance energy-transfer form.)

Typically, the IDA is utilized in the evaluation of this Coulombic interaction. At this level of approximation, the transition density is represented in terms of a basis set of multipolar transition moments of which only the leading, dipole term is used. The dipole transition moment (or transition dipole) has the form $\mu_N^{\mathrm{eq}} = \langle \Psi_{N\mathrm{e}}|\mathbf{r}|\Psi_{N\mathrm{g}}\rangle$ where $\boldsymbol{r}$ is the dipole moment operator. The Coulombic interaction between donor and acceptor transition dipoles is given by the dipole−dipole interaction:

$$V^{\mathrm{d-d}} = \frac{1}{4\pi\epsilon_0}\kappa\frac{|\mu_{\mathrm{D}}||\mu_{\mathrm{A}}|}{R^3} \tag{3}$$

in which the magnitudes of the transition dipoles are contained in $|\mu_{\mathrm{D}}|$ and $|\mu_{\mathrm{A}}|$ and the orientational information is contained in the center-to-center separation, R, and the orientation factor $\kappa \equiv \hat{\mathbf{r}}_{\mathrm{D}}\cdot\hat{\mathbf{r}}_{\mathrm{A}} - 3(\hat{\mathbf{r}}_{\mathrm{D}}\cdot\hat{\mathbf{R}})(\hat{\mathbf{r}}_{\mathrm{A}}\cdot\hat{\mathbf{R}})$ where $\hat{\mathbf{R}}$ is a unit vector connecting the centers of the transition moments and the $\hat{\mathbf{r}}_{\mathrm{N}}$ are unit vectors in the directions of the transition dipoles.

A more accurate description of the Coulombic interaction between transition densities would involve the use of more, or all, of the terms from the multipolar basis set. The multipole expansion is derived from a "two-center" expansion of the $1/r$ interaction term of eq 1 in terms of spherical harmonics.[19−21] Provided the transition densities of the donor and acceptor do not overlap, the Coulombic coupling of eq 1 may be expressed in terms of the multipole transition interaction between the transition densities of the molecules,[22] $V^{\mathrm{Coul}} = V^{\mathrm{mult}} = V^{\mathrm{d-d}} + V^{\mathrm{d-q}} + V^{\mathrm{q-d}} + V^{\mathrm{d-o}} + V^{\mathrm{o-d}} + V^{\mathrm{q-q}} + \ldots$ where $V^{\mathrm{d-d}}$, $V^{\mathrm{d-q}}$, ... denote dipole−dipole, dipole−quadrupole, etc., coupling contributions to the *exact* coupling V^{Coul}. The higher multipole transition moments may be determined in an analogous manner to the dipole transition moment[23,24] (for example, for electric quadrupole transitions, $\Theta_{\alpha\beta}^{\mathrm{eg}} = \langle\Psi_{\mathrm{e}}|r_\alpha r_\beta|\Psi_{\mathrm{g}}\rangle$, or for magnetic dipole transitions, $m_\alpha^{\mathrm{eg}} = \langle\Psi_{\mathrm{e}}|(r \times p)_\alpha|\Psi_{\mathrm{g}}\rangle$). Use of the full multipole interaction accounts for the shape and spatial extent of the transition density of the donor and acceptor but is valid only when the donor and acceptor transition densities are nonoverlapping.

In this work, we demonstrate a practical method for accurately calculating the Coulombic coupling between donor and acceptor transitions. In this method, we define a TDC which is constructed analogously to the continuous transition density of eq 2 by integrating the product of electronic ground and excited states into a three-dimensional grid of finite-sized volume elements (cells) which make up the cube,

$$M_N^{\mathrm{eq}}(x,y,z) = V_\delta \int_z^{z+\delta_z}\int_y^{y+\delta_y}\int_x^{x+\delta_x}\int_s \Psi_{N\mathrm{g}}\Psi^*_{\mathrm{Ne}}\, \mathrm{ds}\, \mathrm{d}x\, \mathrm{d}y\, \mathrm{d}z \tag{4}$$

in which s represents the spin variables, the δ_α define the grid size of the density cube, and V_δ is the element volume ($V_\delta = \delta_x\delta_y\delta_z$) needed as a practical means of converting charge density per unit volume into charge density per element. For the TDCs used here, the elements are defined in terms of Cartesian coordinates in which the δ_x, δ_y, and δ_z are nondivisible step sizes along the respective coordinate axes. Note that any coordinate system could be chosen to define the TDC and that neither the individual elements nor the total TDC need be actually cube-shaped.

The Coulombic coupling is expressed in transition density formalism by McWeeny (eq 14.6.8)[25] which we adapt to our TDCs.

$$V^{\mathrm{Coul}} \cong \sum_{i,j}\frac{M_{\mathrm{D}}^{\mathrm{eg}}(i)\, M_{\mathrm{A}}^{\mathrm{eq}}(j)}{4\pi\epsilon_0 r_{ij}} \tag{5}$$

where $M_{\mathrm{D}}^{\mathrm{eg}}(i)$ and $M_{\mathrm{A}}^{\mathrm{eq}}(j)$ are TDC elements i and j for the donor and acceptor and r_{ij} is their separation as shown in Figure 1. The only approximations involved here are in the graining of

space over which the summation is carried out (i.e., the finite size of the density cube elements) and the level of accuracy of the wave functions from which the TDCs are constructed. Also, as opposed to the multipole expansion, the TDC method is valid at all molecular separations. There is no need to define a molecular separation (center to center or otherwise) as all orientational effects are accounted for in eq 5.

The transition dipoles (and higher order moments) may be recovered from the TDC by defining an origin (which will become the center of the transition dipole) and applying the dipole moment operator

$$\mu_\alpha^{eq} \cong \sum_i r_\alpha M^{eq}(i) \tag{6}$$

where r_α is the vector pointing from the origin to *(x,y,z)*—the location of the TDC element *i*. This form of the dipole transition moment is equivalent to that given earlier except for the graining of space in the TDC. The dipole−dipole coupling, along with the orientation factor, may then be calculated as usual or, alternatively, by rewriting eq 5 in terms of the IDA (or rewriting eq 3 in terms of TDCs)

$$V^{d-d} = \sum_{i,j} M_D^{eq}(i)\, M_A^{eg}(j) r_i r_j V_{DA} \tag{7}$$

where V_{DA} is the dipole coupling tensor,[16] containing distance and orientation dependence through **R** and κ. This is most easily demonstrated by considering the interaction between two classical (static) dipoles.[19−21,26,27] Inspection of Figure 1 reveals that, although the separation r_{ij} is not included explicitly in eq 7, it is accounted for indirectly via the vectors $\mathbf{r}_i$, $\mathbf{r}_j$, and **R**. Use of eq 7 is equivalent to use of the standard dipole−dipole coupling formula (eq 3) with transition dipoles taken from eq 6.

3. Computational Methods

TDCs were obtained via ab initio molecular orbital calculations for individual molecules, carried out with the Gaussian 94 program.[28] Excited-state wave functions were obtained using configuration interaction with single excitations from a spin-restricted Hartree−Fock (RHF) reference determinant (CI-singles, CIS method[29]). The 3-21G* basis set[30] was employed. The geometry of the Bchla and RG were taken from the crystal structure data from the bacterial light-harvesting complex LH2 of *Rhodopseudomonas* (*Rps.*) *acidophila*,[5] with hydrogen atoms added using MNDO optimization (heavy atoms fixed in the crystal structure coordinates).

The transition densities between ground and excited states were generated using the CI-singles wave functions, providing three-dimensional matrices which were used to evaluate eq 5 for the molecules of interest. The integral over space of the TDCs generated by Gaussian 94 was not exactly zero. This residual charge, albeit small (typically 10^{-2} *e*), can affect the calculated couplings. (It adds a first-order electrostatic term, going as R^{-1}, as well as influencing the even multipole transition moments.) To compensate for this, prior to each calculation we add an equal (very small) amount of charge to each element in a given cube to make the integrated charge zero within the accuracy of the computer (typically 10^{-14} *e*).

CIS calculations overestimate the excitation energies and the magnitudes of the transition moments, mainly owing to the neglect of $\sigma-\pi$ dynamic correlation.[31,32] The CIS TDCs provide a reasonable representation of the shape of the transition density, but not the magnitude of its moments. It is impractical to include account of sufficient electron correlation in calculations of the size we have undertaken in the present work; therefore, to obtain quantitative estimations of Coulombic couplings which have relevance to experiment, the CIS transition densities must be scaled. The most salient experimental observables are the multipole transition moments for each electronic transition, of which the dipole transition moment has the dominant magnitude for allowed transitions. Hence, we use a general scaling factor for the TDC elements based on the ratio of the experimental to calculated dipole transition moments: μ^{exp}/μ^{calc}. This scaling factor acts as a correction to the amount of density in each cell of the TDC and could be multiplied through every element of the TDC or simply once to the final value of the coupling. We correct our calculations in LH2 by using μ^{exp} values of 3.29 D for the Bchla Q_x transition,[33] 6.13 D for the Bchla Q_y transition,[33] and 13.0 D for the RG S_2 transition.[34]

The grid size of the density cube may be chosen arbitrarily, thus balancing the computational cost of the coupling calculation with the errors introduced by the graining of space within the density cube. We find the Gaussian 94 default grid size to be quite conservative and the resulting coupling calculations lengthy. For the work here, we employ a coarser graining in which each cube element contains a volume of ~0.23 bohr^3, which is roughly twice the volume of the Gaussian 94 default for RG. We have extensively examined the dependence of calculated coupling strengths on cube element volume (data not shown) and find this coarser size to be well within the bounds of accurate results (<2% error compared to the Gaussian 94 default grid size). However, we have found that calculations performed with very coarse graining (large element volumes) can be misleading, especially at small separations, leading to unpredictable errors of 50% or more in the magnitude of the coupling. Therefore, coarse grid sizes (and hence "monopole" schemes) should be used with caution. To ensure there are no spurious results, we recalculated the coupling of relatively strongly coupled chromophores (V^{Coul} > 50 cm^{-1}) using the Gaussian 94 default density cubes and found no significant discrepancy between the default and the coarser grid size.

4. Results: Couplings in LH2

We have employed the TDC method to determine the Coulombic coupling between various pigments in the LH2 of *Rps. acidophila*, the structure of which has been recently elucidated.[5,35,36] The crystal structure reveals a ring of nine repeat units, or protomers, each of which consists of an α,β-polypeptide pair and its closely associated pigments: two B850 Bchla, one B800 Bchla, and one fully resolved RG molecule. (An additional, partially resolved RG molecule may also be present.) Despite this detailed structural information, the precise energy-transfer mechanism within this antenna system has proven to be enigmatic.[2,8,37−39]

We have calculated Coulombic couplings between RG S_2, B850 Q_y, and B800 Q_y donors and various acceptor states (cf. Table 1). The RG S_2 donor transition is associated with two groups of acceptor transitions: RG S_2, which includes neighboring and next-nearest-neighbor RG molecules, and Bchla, which includes both Q_x and Q_y transitions of all B800 and B850 pigments within ~30 Å of the RG. Thus, the RG−Bchla group includes all EET processes which depopulate the RG S_2 state. The B850 Q_y donor transition comprises only one donor−acceptor group in which the acceptors are the Q_y transitions of all B850 molecules within ~35 Å of the donor. The last two donor−acceptor groups have B800 Q_y as the donor transition and represent B800 to B850 EET, which includes all B850 Q_y

TABLE 1: Values of the Separation, TDC-Derived Orientation Factor (κ, from μ of Eq 6) and Calculated Couplings (V^{Coul} from Eq 5 and V^{d-d} from Eq 7) between the Various Transitions Present in LH2[a]

donor transition	acceptor transition	separation (Å)	κ	V^{Coul} (cm^{-1})	V^{d-d} (cm^{-1})
$RG1_A$ S_2	$RG1_B$ S_2	17.1	0.02	38	37
$RG1_A$ S_2	$RG1_C$ S_2	32.1	0.14	6	4
$RG1_B$ S_2	$\alpha B850_A$ Q_x	28.2	0.70	6	7
$RG1_B$ S_2	$\beta B850_A$ Q_x	21.7	0.48	9	10
$RG1_B$ S_2	$\beta B850_A$ Q_y	21.7	0.24	5	10
$RG1_B$ S_2	$\alpha B850_B$ Q_x	15.9	−0.18	11	−9
$RG1_B$ S_2	$\alpha B850_B$ Q_y	15.9	−0.81	−32	−80
$RG1_B$ S_2	$\beta B850_B$ Q_x	14.2	−1.60	−46	−121
$RG1_B$ S_2	$\beta B850_B$ Q_y	14.2	−0.11	45	−15
$RG1_B$ S_2	$\alpha B850_C$ Q_x	17.1	−1.73	−101	−74
$RG1_B$ S_2	$\alpha B850_C$ Q_y	17.1	0.90	104	72
$RG1_B$ S_2	$\beta B850_C$ Q_x	23.7	−0.77	−16	−12
$RG1_B$ S_2	$\beta B850_C$ Q_y	23.7	−1.81	−80	−54
$RG1_A$ S_2	$\alpha B850_C$ Q_y	29.9	1.71	31	26
$RG1_C$ S_2	$B800_A$ Q_y	30.2	1.17	14	17
$RG1_B$ S_2	$B800_A$ Q_x	13.3	0.39	35	36
$RG1_B$ S_2	$B800_A$ Q_y	13.3	1.64	173	280
$RG1_B$ S_2	$B800_B$ Q_x	10.2	−0.35	−19	−71
$RG1_B$ S_2	$B800_B$ Q_y	10.2	−0.31	−44	−118
$RG1_B$ S_2	$B800_C$ Q_x	27.0	−0.98	−8	−11
$RG1_B$ S_2	$B800_C$ Q_y	27.0	0.50	8	10
$\alpha B850_B$ Q_y	$\alpha B850_A$ Q_y	17.8	−1.43	−46	−48
$\alpha B850_B$ Q_y	$\beta B850_A$ Q_y	9.1	1.11	213	284
$\alpha B850_B$ Q_y	$\beta B850_B$ Q_y	9.5	1.68	238	367
$\beta B850_B$ Q_y	$\beta B850_A$ Q_y	18.6	−1.26	−37	−37
$B800_B$ Q_y	$\alpha B850_A$ Q_y	38.2	−1.18	−4	−4
$B800_B$ Q_y	$\beta B850_A$ Q_y	31.0	1.05	7	7
$B800_A$ Q_y	$\alpha B850_A$ Q_y	23.9	−0.87	−13	−12
$B800_A$ Q_y	$\beta B850_A$ Q_y	18.3	0.13	5	4
$B800_A$ Q_y	$\alpha B850_B$ Q_y	17.6	0.79	27	27
$B800_A$ Q_y	$\beta B850_B$ Q_y	21.8	0.17	23	31
$B800_A$ Q_y	$\alpha B850_C$ Q_y	28.3	−0.55	−4	−5
$B800_A$ Q_y	$\beta B850_C$ Q_y	36.3	1.30	5	5
$B800_B$ Q_y	$B800_C$ Q_y	21.2	−1.33	−27	−26
$B800_A$ Q_y	$B800_C$ Q_y	39.9	−1.04	−3	−3

[a] The labeling scheme of the pigments is depicted in Figure 2. For clarity, transitions in which both V^{Coul} and V^{d-d} are < 10% (5% for RG to Bchla) of the largest V^{Coul} value for each donor−acceptor transition group (e.g., B800−B850 is one donor−acceptor group) are not shown.

transitions within 50 Å of the B800, and B800 to B800 EET, which includes nearest-neighbor and next-to-nearest-neighbor B800 Q_y transitions. Because of rapid Q_x−Q_y internal conversion in Bchla (∼200 fs[40,41]), we have not considered Bchla Q_x transitions as donors. Results of the calculations including center-to-center separations and coupling strengths calculated using both the IDA (eq 7, V^{d-d}) and the density cube method (eq 5, V^{Coul}) are given in Table 1 along with values of the orientation factor, κ, taken from TDC-derived transition dipoles (eq 6). (For Bchla donor types, we have not reported those donor−acceptor pairs with both V^{Coul} and V^{d-d} values less than 10% of the largest V^{Coul} value in the group. For the RG donor type we have withheld those pairs less than 5% of the largest V^{Coul} value.) All chromophore positions utilized for this work come from three adjoining α,β-polypeptide pairs, labeled A, B, and C. Thus, $\alpha B850_A$, $\beta B850_A$, $B800_A$, and $RG1_A$ are all from the same protomer (A) and $\beta B850_A$ adjoins $\alpha B850_B$ as shown in Figure 2.

Both the orientation and separation change as different chromophores around the LH2 ring are considered; it is therefore difficult to characterize coupling differences between the TDC and IDA estimates for various donor and acceptor pairs. In

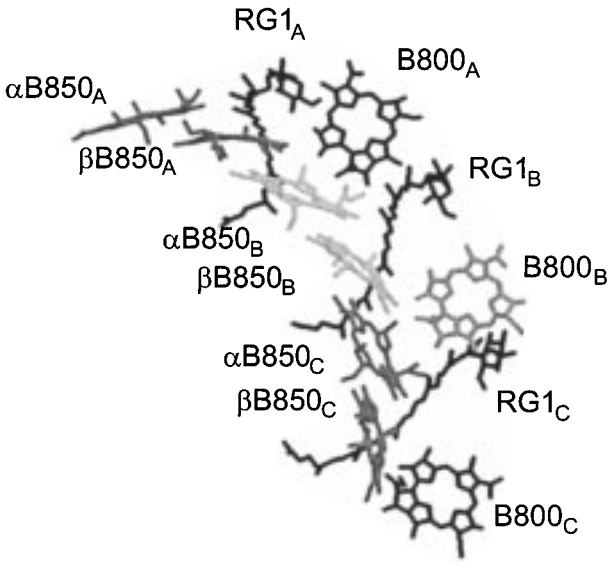

Figure 2. Depiction of the labeling scheme used for the pigments in LH2. One-third of the full ring is shown with the phytyl chains of the Bchla removed for clarity. The carotenoids are shaded black; the B850 Bchla of protomers A and C are gray while those of protomer B are nearly white. The B800 Bchla of protomers A and C are dark gray and the B800 Bchla of protomer B is light gray. The pigments are as seen in the crystal structure of *Rps. acidophila*.[5]

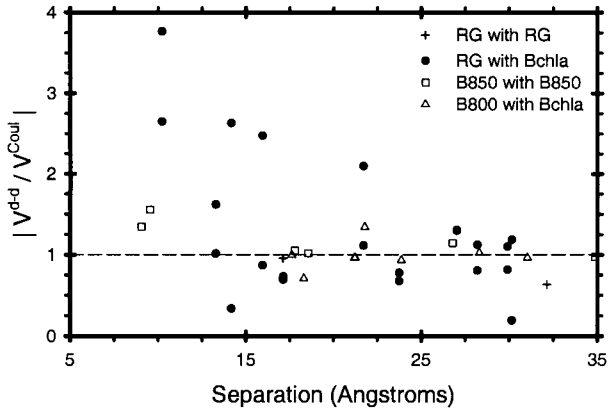

Figure 3. Deviation between the actual Coulombic coupling, V^{Coul}, determined from eq 5 and the ideal dipole approximation to it, V^{d-d}, of eq 7 plotted as the ratio $|V^{d-d}/V^{Coul}|$ versus the center-to-center separation for various pigments in LH2 (values are given in Table 1). Couplings involving two RG pigments are given by pluses (+), while those involving one RG pigment and one Bchla (B850 or B800) pigment are denoted by solid circles (●). Couplings between two B850 Bchla pigments are given by open squares (□), and those involving one B800 Bchla pigment and one Bchla (B850 or B800) pigment are denoted by open triangles (△).

Figure 3, the ratio $|V^{d-d}/V^{Coul}|$ is plotted versus the separation of donor and acceptor. Although there is no marked trend in these data, it is clear that the discrepancy in coupling can reach values on the order of the coupling itself ($V^{d-d}/V^{Coul} \sim 0$ or $\gtrsim 2$) even at separations greater than 20 Å. Moreover, much larger deviations are common for separations less than 20 Å. It is also noteworthy that in some instances the two methods can have remarkable (perhaps fortuitous) agreement at separations as small as 13 Å.

The coupling strengths shown in Table 1 allow determination of EET pathways within donor−acceptor groups (where weak coupling is assumed). Estimating a rate of EET in the weak coupling limit requires only knowledge of the electronic coupling, V, and the spectral overlap, J, between donor and

TABLE 2: Values of the Spectral Overlap Used in Eq 8 and Resulting EET Times (Inverse Rates) between Some of the Donor−Acceptor Pairs Given in Table 1[a]

donor transition	acceptor transition	overlap (10^{-6}cm)	rate^{-1} (ps)	probability (%)
$RG1_B$ S_2	$\beta B850_B$ Q_x	210	1.9	4.4
$RG1_B$ S_2	$\alpha B850_C$ Q_x	210	0.4	21
$RG1_B$ S_2	$B800_A$ Q_x	210	3.3	2.6
$RG1_B$ S_2	$B800_A$ Q_y	16	1.7	4.9
$B800_B$ Q_y	$\beta B850_A$ Q_y	400	45	2.9
$B800_A$ Q_y	$\alpha B850_A$ Q_y	400	13	10
$B800_A$ Q_y	$\beta B850_A$ Q_y	400	72	1.8
$B800_A$ Q_y	$\alpha B850_B$ Q_y	400	2.8	46
$B800_A$ Q_y	$\beta B850_B$ Q_y	400	3.9	33
$B800_A$ Q_y	$\alpha B850_C$ Q_y	400	107	1.2
$B800_A$ Q_y	$\beta B850_C$ Q_y	400	78	1.7

[a] Probability is the probability of the given acceptor to receive EET from the given type of donor (i.e., $B800_A$ Q_y and $B800_B$ Q_y are equivalent donor types) relative to all other possible acceptors within the donor−acceptor group (as in eq 9). Two donor−acceptor groups are given: RG−Bchla (top) and B800 Q_y−B850 Q_y (bottom). An $S_2 \rightarrow S_1$ internal conversion time of 135 fs is also assumed in the RG-Bchla group.

acceptor transitions.

$$k = \frac{4\pi^2}{h^2 c}|V|^2 J \tag{8}$$

Values of the spectral overlap for most pigments under consideration were estimated previously in a study of the B800−B820 LH2 complex of *Rps. acidophila*[42] from which spectral parameters for the RG S_2 and various Bchla transitions can be taken (after shifting the B820 Q_y band to 850 nm). Because the carotenoid emission extends over the entire range of Bchla absorption and because the vibronic features constitute only a small fraction of the total area of the Bchla absorption, for the RG−Bchla spectral overlap the Bchla absorption spectrum can be well-approximated by a single Gaussian. However, spectral overlap between Bchla pigments is quite dependent on the exact shape of the Bchla spectrum. Recently, Pullerits et al. have examined the temperature dependence of the vibronic structure of Bchla transitions and have made upper-limit estimates of the B800−B800 and B800−B850 spectral overlaps (0.0032 and 0.0004, respectively) which we shall use here.[43] Application of the coupling strengths from Table 1 along with the spectral overlaps leads to the EET rate estimates given in Table 2.

By comparing the rates of all processes by which energy leaves a particular donor, we can estimate the relative probability of a particular acceptor to receive EET from that donor. The probability of transfer to acceptor *i* is the rate of EET to *i* divided by the total of all rates k_j which depopulate the donor.

$$P_i = k_i / \sum_j k_j \tag{9}$$

The k_j include EET from the donor to all acceptors in the donor−acceptor group as well as other nonradiative and radiative processes. As we are primarily concerned with the relative probabilities of each of the acceptors within a donor−acceptor group to receive EET from the donor and most other processes present in the system have comparatively small rates, we will include only the EET rates calculated here in the k_j of eq 9. One important exception is the S_2-S_1 internal conversion of RG. (See papers by Koyama et al. and Frank and Cogdell for descriptions of the singlet states in carotenoids.[3,44]) Because this rapid process (estimated to be 135 fs[42]) dominates the dynamics of the RG S_2 state, it has been included in the k_j. Two donor−acceptor groups are represented in Table 2: RG−Bchla (top) and B800−B850 (bottom), including only those acceptors which have a significant probability (>1%) of receiving excitation.

5. Discussion

We have reported here estimates of the Coulombic contribution to the total electronic couplings between various chromophores present in the LH2 complex of *Rps. acidophila*. Specifically, we have considered the three types of pigments present in LH2: B850 Bchla, B800 Bchla, and the carotenoid, RG. Coulombic couplings were calculated between various pigment transitions over a wide range of center-to-center separations using the TDC method. Provided a sensible spatial cube is chosen (small cells and large boundaries), the accuracy of these calculations is limited only by the quality of ground- and excited-state wave functions. Ideally, these would be calculated using a large basis set and a CAS−SCF method together with a perturbative correction for core-active space dynamic correlation. In this case, the transition density should be well-reproduced, and no correction to the couplings would be required. However, such a calculation is not practical at this time for such large systems. We have instead used the ab initio CI-singles method with a 3-21G* basis set, making a post hoc correction for the electron correlation using a scaling factor. (This is important in order to obtain physically relevant results, as discussed in Section 3.) We believe these results represent the best estimates of the Coulombic couplings reported to date. Short-range couplings (i.e., contributions that depend explicitly on orbital overlap) are not calculated here. We have determined these using more complex calculations, as they are significant for the interactions within the B850 ring. However, they have no significant bearing on the results discussed in the present work and are presented in detail elsewhere.[45]

In addition to calculating reliable estimates of the couplings, we investigated the usefulness of the dipole approximation. Comparison of results from the TDC method to the IDA method (Figure 3) suggests that for many of the interactions within LH2, the IDA gives poor values for the coupling strengths. The largest discrepancies between V^{d-d} and V^{Coul} involve the RG molecule, while couplings involving the B800 Bchla molecules give consistently similar results. The structure of RG provided by the crystallographic data is far from symmetric; the backbone of the carotenoid winds around the polypeptides and Bchla molecules.[36] Thus, the associated electronic transition density, shown in Figure 4, cannot realistically be represented by a dipole transition moment. Furthermore, the spatial extent of the transition is quite large (roughly 25 Å end to end). Both of these factors increase the significance of higher order terms of the multipole expansion of the coupling compared to the dipole−dipole term. This slow convergence of the multipole expansion most likely arises because there is no point about which to expand the spherical harmonics of the multipole expansion for the RG transition density (e.g., there is no center of symmetry within the RG transition density). As demonstrated by the calculations and shown in Figure 3, this effect can be significant at separations (R > 20 Å) where the IDA might be considered to be reasonable. As separations become smaller (R < 20 Å), deviations from the IDA become much larger than the value of the coupling itself.

The B800 Bchla couplings are found to be well described by the IDA even though nearest-neighbor separations are quite small (less than 2*l*). The B800 structure and hence the transition

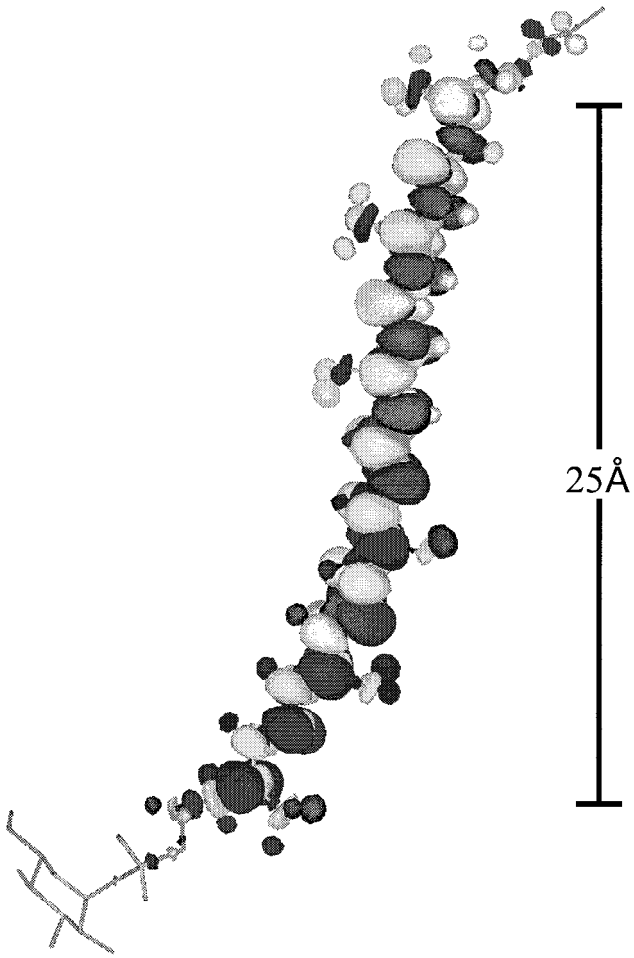

Figure 4. Transition density for the carotenoid, RG, used in the LH2 coupling calculations. The shape of the carotenoid is from the crystal structure[5] as described in the text. The transition density is determined using Gaussian 94[28] as described in the text.

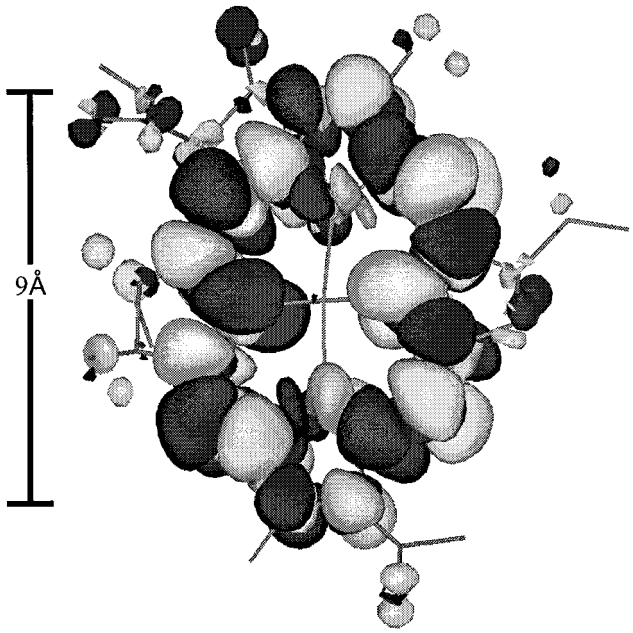

Figure 5. Transition density for the B800 Bchla used in the LH2 coupling calculations. The shape of the Bchla is from the crystal structure[5] as described in the text. The transition density is determined using Gaussian 94[28] as described in the text.

density are quite symmetric, as shown in Figure 5. Therefore, we expect that a multipole expansion should be quickly convergent despite the fact that the B800 transition density is spatially quite large (~9 Å in diameter).

Of particular interest within LH2 are the EET rates within a donor−acceptor group, as they relate to experiment. The sum of all the RG to Bchla EET rates, along with the S_2-S_1 internal conversion rate gives the depopulation rate of the RG S_2 state (assuming that other nonradiative and radiative rates are negligible). We estimate that depopulation of the RG S_2 state occurs on a time scale of 85fs by using the EET rates calculated here and a "transfer time" of 135 fs[42] for the S_2-S_1 internal conversion. This agrees well with the 50−100 fs depopulation times reported by several groups[42,46,47] on similar complexes. However, because the rapid internal conversion dominates the S_2 depopulation, a wide range of calculated RG−Bchla rates lie within the range of experiment.

In these calculations, we have rather naively treated the B850 pigments as individual chromophores, which is not an accurate depiction of the true electronic nature of the B850 ring. The extent of delocalization in this ring is not known, but recent work indicates that, on time scales relevant to energy transfer, the electronic states of the B850 ring are delocalized over 2−4 monomers, suggesting that a ring of 9 dimers (or fewer multimers) would be a better representation than a ring of 18 monomers.[48−51] An analysis accounting for the excitonic nature of the B850 ring is outside of the scope of this paper; however, details of the RG to B850 couplings given in the present work form a basis for such a treatment. (The rates, on the other hand, should be used only as a guide.)

A summary of the interaction between the $RG1_B$ S_2 transition and neighboring Bchla transitions is given in Figure 6A. The Coulombic couplings given here suggest that the $RG1_B$ S_2 transition couples most strongly to both the Q_x and Q_y transitions of the neighboring $\alpha B850_C$, although because of larger spectral overlap the Q_x transition is by far the "preferred" energy acceptor. This $RG1_B$ $S_2-\alpha B850_C$ Q_x energy transfer is the only process that is competitive with S_2-S_1 internal conversion representing 21% of the total while internal conversion claims 63%. However, the $\beta B850_B$ Q_x transition and both the Q_x and Q_y transitions of the $B800_A$ each receive noticeable amounts of the excitation energy and, together, receive 12% of the RG S_2 excitation energy. The coupling of $RG1_B$ S_2 to the $B800_A$ Q_y transition is actually the strongest of the group (173 cm^{-1}) though it yields only 5% of the total EET because of a meager spectral overlap.[42]

Note also, from Table 1, that the calculation of $RG1_B$ S_2-B800_A Q_y coupling and $RG1_B$ $S_2-\alpha B850_C$ Q_x coupling are two cases for which use of the IDA would be especially in error—resulting in a 5-fold change in the relative rates (proportional to the square of the coupling) of these two acceptors compared to the TDC results. Moreover, it is interesting that these two Bchla pigments which couple most strongly to the RG are in fact not the closest pigments measured center-to-center. $B800_A$ is 13.3 Å from $RG1_B$, while $B800_B$ is 10.2 Å; $\alpha B850_C$ is 17.1 Å away, while $\alpha B850_B$ is 15.9 Å and $\beta B850_B$ is 14.2 Å. The large size of the RG transition means that center-to-center separation is not a good indicator of the distance between transitions. Orientation factors are generally small for the $B800_B$, $\alpha B850_B$, and $\beta B850_B$ transitions resulting in poor coupling to RG, except for the $\beta B850_B$ Q_x which has $\kappa = -1.60$. The corresponding V^{d-d} value of −121 cm^{-1} ($RG1_B$ $S_2-\beta B850_B$ Q_x) is the largest RG−B850 interaction; however, higher multipole effects reduce V^{Coul} to −46 cm^{-1}. Such an effect is not unique; as mentioned earlier, many of the calculated

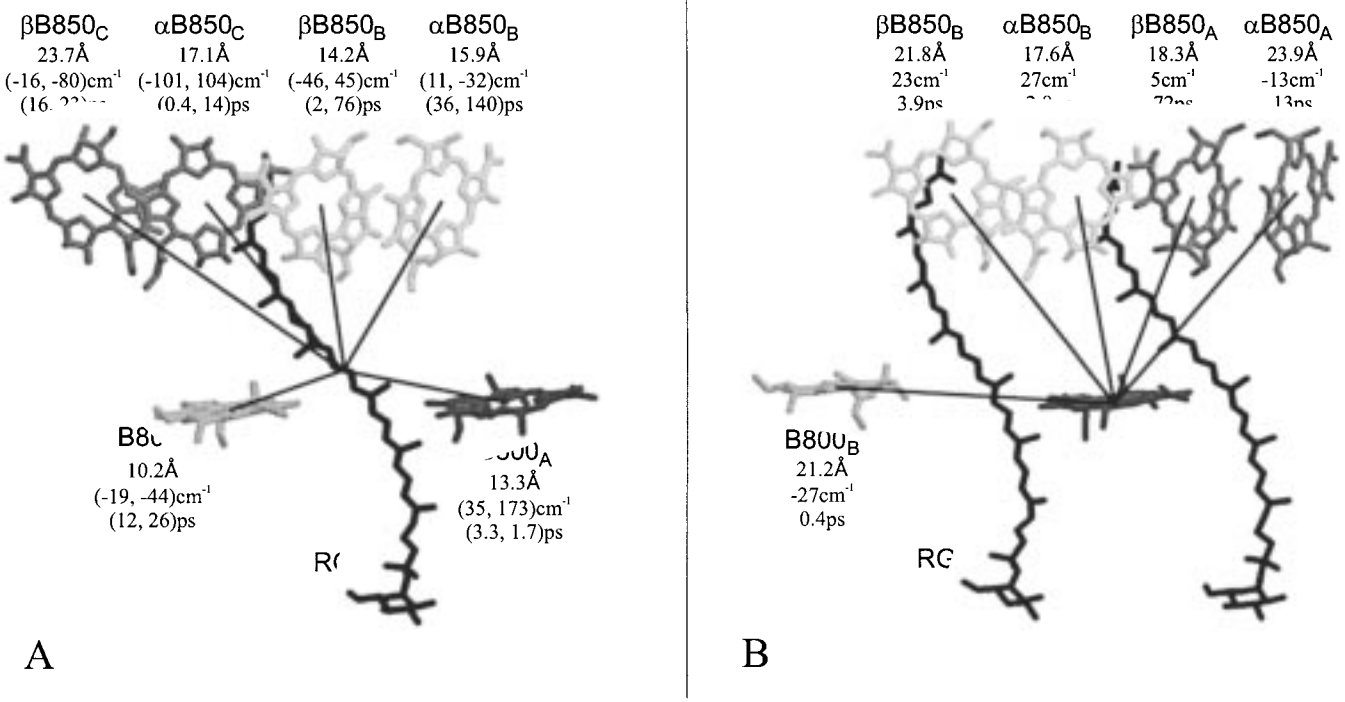

Figure 6. Coupling strengths and energy transfer times from the $RG1_B$ S_2 (A) and $B800_A$ Q_y (B) transitions to nearby Bchla transitions. Shading of the chromophores is as in Figure 2. Near each acceptor pigment is given the label, center-to-center separation, coupling strength V^{Coul}, and transfer time. For transfer from RG S_2, the interaction with both the Q_x and Q_y transitions of the acceptor is given (Q_x, Q_y), whereas for B800 Q_y only interaction with the acceptor Q_y transition is given.

couplings involving RG show large discrepancies between the TDC and IDA methods.

Because our simple treatment of the B850 pigments lacks orbital overlap effects which must be considered when examining the *total coupling* between these pigments, we will not give an extended discussion of coupling strengths between them in the present work. However, the results reported here are relevant within a discussion of *Coulombic coupling*. The TDC method yields coupling strengths of 238 cm^{-1} within the intraprotomer $\alpha-\beta$ pair and 213 cm^{-1} within the interprotomer $\beta-\alpha$ pair. These values are significantly smaller in magnitude than the IDA results, indicating a strong influence from higher multipole moments. We find dipole−dipole coupling strengths (V^{d-d}) of 367 cm^{-1} within the intraprotomer $\alpha-\beta$ pair and 284 cm^{-1} within the interprotomer $\beta-\alpha$ pair which are similar to those given by Pullerits et al., who find 410 cm^{-1} within the intraprotomer $\alpha-\beta$ pair and 310 cm^{-1} within the interprotomer $\beta-\alpha$ pair.[43] It is not surprising that the dipole−dipole results given here and those of ref 43 yield slightly different results because transition dipoles derived from the calculated transition densities are slightly different than those of Pullerits et al., which were established from structural parameters (pointing from N to N). As may be expected, monopole calculations by Sauer et al., which are intermediate to the TDC and IDA methods in accounting for the shape of the transition density, give an intermediate coupling strength of 273 cm^{-1} within the intraprotomer $\alpha-\beta$ pair.[52]

Examination of the B800 to B850 energy-transfer times (summarized in Figure 6B) suggests a total B800−B850 transfer of 1.3 ps, substantially slower than the 650−700 fs seen experimentally[8,43,53] in the LH2 of *Rhodobacter sphaeroides*. In the recent work by Pullerits et al. they calculated an even slower 1.9 ps for the transfer from a single B800 to the nearest four B850 pigments.[43] Here we find coupling strengths which, after squaring and summing, are slightly larger in magnitude (27, −23, −13, and 5 cm^{-1} compared to 29, 13, 7, and 6 cm^{-1} from Pullerits et al.), in addition to significant coupling to several other B850 molecules (7, 5, −4, −4, −3, and −3 cm^{-1}). Thus, our total B800−B850 EET rate is 30% larger than that found by Pullerits et al., although it is still a factor of 2 slower than experiment.

It was suggested by Pullerits et al. that carotenoid-mediated superexchange from B800 to B850 may account for the bulk of the difference in rates. In other words, the transition densities of the donor and acceptor are coupled via the carotenoid $S_2 \leftarrow S_0$ transition density. We have performed preliminary calculations using second-order perturbation theory [$V^{SE} = -V_{B800-RG}V_{RG-B850}/(E_{RG} - E_{B800})$] to estimate the superexchange contribution to the $B800_A$−B850 coupling via the $RG1_B$ S_2 transition. The 0−0 energy gap is taken to be that reported by Krueger et al. for RG, 6400 cm^{-1}.[42] These results suggest that the carotenoid mediates a minimal additional coupling of 2−3 cm^{-1} between $B800_A$ Q_y and both the α and β $B850_C$ Q_y. The small magnitudes of the superexchange-mediated couplings compared to the Coulombic couplings suggest that the carotenoid plays only a minor role in the B800−B850 *Coulombic* energy transfer. However, it is possible that short-range interactions (orbital overlap dependent) could significantly enhance the RG−B850 coupling strengths and thus affect the superexchange rate. In other words, mixing of the RG and B850 orbitals could have a large influence on the B800−B850 coupling.[12,54−57] We are currently conducting a detailed investigation of these effects and have preliminary results which indicate that some B850 electron density extends down the conjugated chain of the carotenoid.[58] In any event, it is interesting that the RG appears to be most capable of promoting EET from B800 to the B850 of a *next-to-nearest-neighbor* protomer ($B800_A$ to $\alpha B850_C$).

The transfer of energy across protomer boundaries is well represented in Table 2. The RG transfers mainly to three different pigments, each of which resides in a different protomer. The B800 Bchla transfers mainly to four different pigments (including other B800s) in three different protomers. This reveals that energy transfer efficiency is maximized by having several viable acceptors for every donor pigment. While recent photon echo peak shift measurements on LH1 suggest that the $\alpha-\beta$ dimer provides a reasonable description of the *electronic structure* of the (B850) ring on time scales relevant to energy transfer,[48] the presence of significant interprotomer energy-transfer pathways found in this work suggests that these pathways must be considered when describing *light-harvesting function*.

The rapid (<400 fs) B800−B800 energy transfer resulting from our calculation is similar to estimates by Pullerits et al.[43] There have been conflicting reports on the rate of B800−B800 transfer in LH2.[8,43,59−63] The calculations in this work suggest that, at least in complexes that share the *Rps. acidophila* structure, rapid B800−B800 transfer does occur. Note that the coupling between the B800 pigments is moderate (<30 cm^{-1}); it is the large spectral overlap that provides the impetus for rapid EET.

6. Conclusions

A general approach for calculating the Coulombic coupling between closely interacting or weakly allowed transition densities of donor and acceptor has been described and employed to investigate the Coulombic coupling within bacterial light-harvesting antenna. Transition densities of donor and acceptor were generated from ab initio CI-singles wave functions as three-dimensional grids. It was demonstrated that the multipolar expansion relevant to the Coulombic interaction may be determined to infinite order using the Coulombic coupling (eq 5) between transition density cubes (TDCs), as described in the present work. In addition, the TDC method is applicable at all interchromophore separations while the multipole expansion (as well as the dipole−dipole limit) is only valid at separations beyond the van der Waals radii of donor and acceptor.

EET rates within LH2, estimated using coupling strengths from the TDC method, suggested that both RG and B800 Bchla transfer energy within and across α,β-polypeptide pair boundaries. Estimation of the RG S_2 depopulation time scale of 85 fs agrees well with experimental results, while estimation of the total B800−B850 transfer time of 1.3 ps (2 times slower than experiment) implies that the excitonic character of the B850 ring along with orbital overlap effects and perhaps superexchange should be considered for these chromophores. Significant coupling and a large spectral overlap[43] between B800 Bchlas also suggest that rapid B800−B800 transfer may occur. (We have not considered the carotenoid S_1 transition in this work.) The present work has indicated that both RG and B800 Bchla pigments transfer energy across protomer unit boundaries, suggesting that energy-transfer pathways between protomer units are important in LH2 function.

Acknowledgment. This work was initiated at The University of Chicago and was supported by a grant from the NSF. B.K. was supported as a Department of Defense fellow.

References and Notes

(1) van Grondelle, R.; Dekker, J. P.; Gillbro, T.; Sundström, V. *Biochim. Biophys. Acta* **1994**, *1187*, 1−65.

(2) Pullerits, T.; Sundström, V. *Acc. Chem. Res.* **1996**, *29*, 381−389.

(3) Frank, H. A.; Cogdell, R. J. *Photochem. Photobiol.* **1996**, *63*, 257−264.

(4) Kühlbrandt, W. *Structure* **1995**, *3*, 521−525.

(5) McDermott, G.; Prince, S. M.; Freer, A. A.; Hawthornthwaite-Lawless, A. M.; Papiz, M. Z.; Cogdell, R. J.; Isaacs, N. W. *Nature* **1995**, *374*, 517−521.

(6) Koepke, J.; Hu, X.; Muenke, C.; Schulten, K.; Michel, H. *Structure* **1996**, *4*, 581−597.

(7) Bradforth, S. E.; Jimenez, R.; van Mourik, F.; van Grondelle, R.; Fleming, G. R. *J. Phys. Chem.* **1995**, *99*, 16179−16191.

(8) Jimenez, R.; Dikshit, S. N.; Bradforth, S. E.; Fleming, G. R. *J. Phys. Chem.* **1996**, *100*, 6825−6834.

(9) Förster, T. Delocalized Excitation and Excitation Transfer. In *Modern Quantum Chemistry*; Sinanoglu, O., Ed.; Academic Press: New York, 1965; Vol. III, pp 93−137.

(10) Agranovich, V. M.; Galanin, M. D. In *Electronic Excitation Energy Transfer in Condensed Matter*; Agranovich, V. M., Maradudin, A., Eds.; North-Holland: Amsterdam, 1982.

(11) Speiser, S. *Chem. Rev.* **1996**, *96*, 1953.

(12) Scholes, G. D.; Harcourt, R. D. *J. Chem. Phys.* **1996**, *104*, 5054−5061.

(13) Scholes, G. D.; Ghiggino, K. P. In *Advances in Multiphoton Processes and Spectroscopy*; Lin, S. H., Villaeys, A. A., Fujimura, Y., Eds.; World Scientific: Singapore, 1996; Vol. 10, pp 95−331.

(14) Scholes, G. D.; Harcourt, R. D.; Ghiggino, K. P. *J. Chem. Phys.* **1995**, *102*, 9574−9581.

(15) Harcourt, R. D.; Scholes, G. D.; Ghiggino, K. P. *J. Chem. Phys.* **1994**, *101*, 10521−10525.

(16) Andrews, D. L. *Chem. Phys.* **1989**, *135*, 195.

(17) Chang, J. C. *J. Chem. Phys.* **1977**, *67*, 3901−3909.

(18) Philipson, K. D.; Tsai, S. C.; Sauer, K. *J. Phys. Chem.* **1971**, *75*, 1440−1445.

(19) Hirschfelder, J. O.; Curtis, C. F.; Bird, R. B. *Molecular Theory of Gases and Liquids*; John Wiley and Sons: New York, 1954.

(20) Buehler, R. J.; Hirschfelder, J. O. *Phys. Rev.* **1951**, *83*, 628.

(21) Buehler, R. J.; Hirschfelder, J. O. *Phys. Rev.* **1952**, *85*, 149.

(22) Scholes, G. D.; Andrews, D. L. *J. Chem. Phys.* **1997**, *107*, 5374−5384.

(23) Craig, D. P.; Thirunamachandran, T. *Molecular Quantum Electrodynamics*; Academic Press: New York, 1984.

(24) Struve, W. S. *Fundamentals of Molecular Spectroscopy*; Wiley: New York, 1989.

(25) McWeeny, R. *Methods of Molecular Quantum Mechanics*, 2nd ed.; Academic Press: London, 1992.

(26) Buckingham, A. D. In *Intermolecular Forces—from Diatomics to Biopolymers*; Pullman, B., Ed.; Wiley: New York, 1978.

(27) Stone, A. J. In *Theoretical Models of Chemical Bonding*; Maksic, Z. B., Ed.; Springer-Verlag: Berlin, 1991; Vol., Part 4.

(28) Gaussian 94, Revision D.4: Frisch, M. J.; Trucks, G. W.; Schlegel, H. B.; Gill, P. M. W.; Johnson, B. G.; Robb, M. A.; Cheeseman, J. R.; Keith, T.; Petersson, G. A.; Montgomery, J. A.; Raghavachari, K.; Al-Laham, M. A.; Zakrzewski, V. G.; Ortiz, J. V.; Foresman, J. B.; Cioslowski, J.; Stefanov, B. B.; Nanayakkara, A.; Challacombe, M.; Peng, C. Y.; Ayala, P. Y.; Chen, W.; Wong, M. W.; Andres, J. L.; Replogle, E. S.; Gomperts, R.; Martin, R. L.; Fox, D. J.; Binkley, J. S.; Defrees, D. J.; Baker, J.; Stewart, J. P.; Head-Gordon, M.; Gonzalez, C.; Pople, J. A.; Gaussian Inc.; Pittsburgh, PA, 1995.

(29) Foresman, J. B.; Head-Gordon, M.; Pople, J. A.; Frisch, M. J. *J. Phys. Chem.* **1992**, *96*, 135.

(30) Hariharan, P. C.; Pople, J. A. *Theor. Chim. Acta* **1973**, *28*, 213.

(31) Matos, J. M. O.; Roos, B. O.; Malmqvist, P.-A. *J. Chem. Phys.* **1987**, *86*, 1458.

(32) Matos, J. M. O.; Roos, B. O. *Theor. Chim. Acta* **1988**, *74*, 363.

(33) Sauer, K.; Lindsay Smith, J. R.; Schultz, A. J. *J. Am. Chem. Soc.* **1966**, *88*, 2681−2688.

(34) Andersson, P. O.; Gillbro, T.; Ferguson, L.; Cogdell, R. J. *Photochem. Photobiol.* **1991**, *54*, 353−360.

(35) Prince, S. M.; Papiz, M. Z.; Freer, A. A.; McDermott, G.; Hawthornthwaite-Lawless, A. M.; Cogdell, R. J.; Isaacs, N. W. *J. Mol. Biol.* **1997**, *268*, 412−423.

(36) Freer, A.; Prince, S.; Sauer, K.; Papiz, M.; Hawthornthwaite-Lawless, A.; McDermott, G.; Cogdell, R.; Isaacs, N. *Structure* **1996**, *4*, 449−462.

(37) Pullerits, T.; Chachisvillis, M.; Sundström, V. *J. Phys. Chem.* **1996**, *100*, 10787−10792.

(38) Kuehn, O.; Chernyak, V.; Mukamel, S. *J. Chem. Phys.* **1996**, *105*, 8586.

(39) Meier, T.; Chernyak, V.; Mukamel, S. *J. Chem. Phys.* **1997**, *107*, 8759−8780.

(40) Ganago, A. O.; Parker, E. P.; Laible, P. D.; Albrecht, A. C.; Owens, T. G. *Laser Phys.* **1995**, *5*, 693−698.

(41) Du, M.; Rosenthal, S. J.; Xie, X.; DiMagno, T. J.; Schmidt, M.; Hanson, D. K.; Schiffer, M.; Norris, J. R.; Fleming, G. R. *Proc. Natl. Acad. Sci. U.S.A.* **1992**, *89*, 8517−8521.

(42) Krueger, B. P.; Scholes, G. D.; Jimenez, R.; Fleming, G. R. *J. Phys. Chem. B* **1998**, *102*, 2284−2292.

(43) Pullerits, T.; Hess, S.; Herek, J. L.; Sundström, V. *J. Phys. Chem. B* **1997**, *101*, 10560−10567.

(44) Koyama, Y.; Kuki, M.; Andersson, P. O.; Gillbro, T. *Photochem. Photobiol.* **1996**, *63*, 243−256.

(45) Scholes, G. D.; Gould, I. R.; Fleming, G. R. Unpublished results.

(46) Ricci, M.; Bradforth, S. E.; Jimenez, R.; Fleming, G. R. *Chem. Phys. Lett.* **1996**, *259*, 381−390.

(47) Andersson, P. O.; Cogdell, R. J.; Gillbro, T. *Chem. Phys.* **1996**, *210*, 195−217.

(48) Yu, J. Y.; Nagasawa, Y.; van Grondelle, R.; Fleming, G. R. *Chem. Phys. Lett.* **1997**, *280*, 404−410.

(49) Monshouwer, R.; Abrahamsson, M.; van Mourik, F.; van Grondelle, R. *J. Phys. Chem. B* **1997**, *101*, 7241−7248.

(50) Alden, R. G.; Johnson, E.; Nagarajan, V.; Parson, W. W.; Law, C. J.; Cogdell, R. G. *J. Phys. Chem. B* **1997**, *101*, 4667−4680.

(51) Chachivilis, M.; Kühn, O.; Pullerits, T.; Sundström, V. *J. Phys. Chem. B* **1997**, *101*, 7275−7283.

(52) Sauer, K.; Cogdell, R. J.; Prince, S. M.; Freer, A.; Isaacs, N. W.; Scheer, H. *Photochem. Photobiol.* **1996**, *64*, 564−576.

(53) Shreve, A. P.; Trautman, J. K.; Frank, H. A.; Owens, T. G.; Albrecht, A. C. *Biochim. Biophys. Acta* **1991**, *1058*, 280−288.

(54) Scholes, G. D.; Ghiggino, K. P.; Oliver, A. M.; Paddon-Row, M. N. *J. Phys. Chem.* **1993**, *97*, 11871.

(55) Newton, M. D. *Chem. Rev.* **1991**, *91*, 767−792.

(56) Bixon, M.; Jortner, J.; Michelbeyerle, M. *Chem. Phys.* **1995**, *197*, 389−404.

(57) Clayton, A. H. A.; Scholes, G. D.; Ghiggino, K. P.; Paddon-Row, M. N. *J. Phys. Chem.* **1996**, *100*, 10912−10918.

(58) Scholes, G. D.; Gould, I. R.; Krueger, B. P.; Fleming, G. R. Unpublished results.

(59) Monshouwer, R.; Ortiz de Zarate, I.; van Mourik, F.; van Grondelle, R. *Chem. Phys. Lett.* **1995**, *246*, 341−346.

(60) Joo, T.; Jia, Y.; Yu, J.-Y.; Jonas, D. M.; Fleming, G. R. *J. Phys. Chem.* **1996**, *100*, 2399−2409.

(61) Kramer, H. J. M.; van Grondelle, R.; Hunter, C. N.; Westerhuis, W. H. J.; Amesz, J. *Biochim. Biophys. Acta* **1984**, *765*, 156−165.

(62) De Caro, C.; Visschers, R. W.; van Grondelle, R.; Völker, S. J. *J. Phys. Chem.* **1994**, *98*, 10584−10590.

(63) Hess, S.; Åkesson, E.; Cogdell, R. J.; Pullerits, T.; Sundström, V. *Biophys. J.* **1995**, *69*, 2211−2225.

ADDITIONS AND CORRECTIONS

1997, Volume 101B

Akira Sasahara,* Hiroyuki Tamura, and Ken-ichi Tanaka: Catalytic Activity of Pt-Deposited Rh(110) Bimetallic Surface for NO + H_2 Reaction

Pages 1186 and 1188. All of the notation of the "c(2×2)" LEED pattern for the Pt/Rh(110) reconstruction by oxygen should be "c(2×4)".

Published on Web 10/28/1998

1998, Volume 102B

Brent P. Krueger, Gregory D. Scholes, and Graham R. Fleming*: Calculation of Couplings and Energy-Transfer Pathways between the Pigments of LH2 by the ab Initio Transition Density Cube Method

Page 5384. Figure 6 was published in an unacceptable form. A corrected version is shown below.

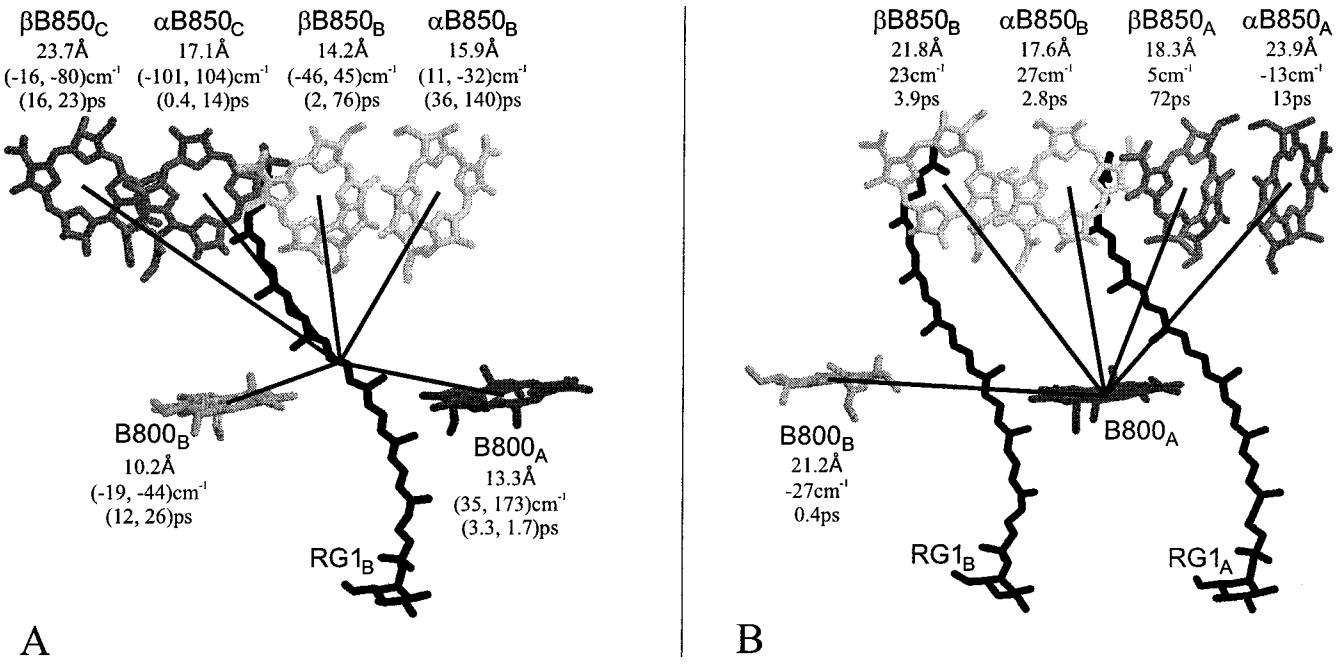

Published on Web 10/28/1998